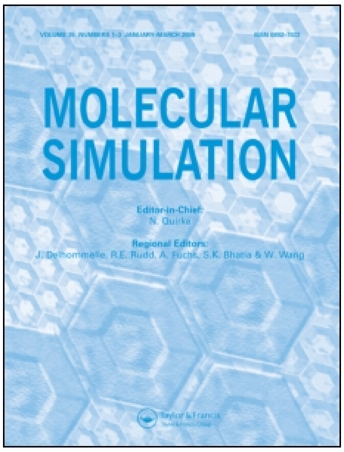

Molecular Simulation
Publication details, including instructions for authors and subscription information:
http://www.informaworld.com/smpp/title~content=t713644482

Fluctuation Simulations and the Calculation of Mechanical Partial Molar Properties

Pablo G. Debenedetti[a]
[a] Department of Chemical Engineering, Princeton University, Princeton, NJ, USA

To cite this Article Debenedetti, Pablo G.(1989) 'Fluctuation Simulations and the Calculation of Mechanical Partial Molar Properties', Molecular Simulation, 2: 1, 33 — 53

To link to this Article: DOI: 10.1080/08927028908032782

URL: http://dx.doi.org/10.1080/08927028908032782

Molecular Simulation, 1989, Vol. 2, pp. 33–53
Reprints available directly from the publisher
Photocopying permitted by license only

FLUCTUATION SIMULATIONS AND THE CALCULATION OF MECHANICAL PARTIAL MOLAR PROPERTIES

PABLO G. DEBENEDETTI

Department of Chemical Engineering, Princeton University, Princeton, NJ 08544, USA

(Received December, 1987; in final form March, 1988)

A method for the direct calculation of partial molar volumes, energies, and enthalpies in multicomponent mixtures in which all species have finite concentrations is presented. The approach, which is based on fluctuation theory, allows the simultaneous determination of the properties of all components in the mixture. The advantages and limitations of the method are illustrated through the (N, U, V) molecular dynamics calculation of the mechanical partial molar properties of two binary Lennard-Jones mixtures.

KEY WORDS: Partial molar properties, fluctuations, molecular dynamics, grand canonical ensemble.

1. INTRODUCTION

Partial molar properties are defined generically as

$$\bar{\lambda}_j = \left(\frac{\partial \lambda}{\partial N_j}\right)_{T,P,N[j]} \tag{1}$$

where λ is an extensive quantity, and $N[j]$ denotes constancy of all N_i (moles or molecules) except for N_j ($i, j = 1, \ldots, n$). Mechanical partial molar properties (partial molar volumes, energies, enthalpies) are the natural quantities in terms of which many thermal and volumetric properties of mixtures can be described. The temperature and pressure dependence of the solubility of a pure solute in a mixture, for example, are both functions of the solute's mechanical partial molar properties in the given mixture; heat effects and volume changes on mixing are linear combinations of mechanical partial molar properties; the unusual nature of the environment surrounding solute molecules in dilute mixtures in the vicinity of the solvent's critical point was first discussed in connection with experimental measurements of partial molar volumes of organic solutes in supercritical fluids [1, 2]. The understanding of partial molar properties from a fundamental molecular perspective is thus of significant practical importance.

The computer calculation of a derivative property such as $\bar{\lambda}_j$ can be performed, in general, in two different ways. In direct differentiation methods [3, 4, 5], the partial derivative in Equation (1) is replaced by the calculation of a difference in λ over two isothermal, isobaric simulations having N_j and $N_j - 1$ molecules, respectively, while the number of molecules of all other species is kept constant. This approach allows exact calculation of infinite dilution partial molar properties [3], which are of particular theoretical significance, for example, in connection with the thermodynamics of dilute supercritical mixtures [6, 7]. In the simplest case (a binary mixture), partial molar properties for both components at finite concentrations can be obtained either by performing a series of simulations, fitting a curve through the calculated λ/N vs. x_1 data [$N = N_1 + N_2$, $x_1 = N_1/N$], and applying the tangent-intercept rule [8], or by performing three isothermal-isobaric runs (a "base case" plus one removal/addition run per species). We are not aware of any reported calculation of partial molar properties at finite concentrations via direct differentiation in the literature.

In this paper we discuss an alternative approach: the fluctuation method [9, 10]. In this technique, a fluctuation-explicit operational definition for the partial molar property is first derived, and the appropriate fluctuations are then simulated. A fluctuation simulation allows the simultaneous calculation of the properties of all components in the mixture under study without numerical interpolation or graphical differentiation; its duration, furthermore, is independent of the number of components in the mixture. Because the calculation of the average of a given quantity takes considerably less computer time than the calculation of the moments of its distribution (for a comparable level of accuracy), the advantages of the fluctuation method (theoretical interest of the operational definitions, computational advantages associated with the simultaneous calculation of properties for all components and with the insensitivity of the simulation's length to the number of components) must be weighed against the longer duration of individual simulations. The operational definitions used here contain a built-in consistency constraint: the equation $\lambda = \sum N_i \bar{\lambda}_i$ (homogeneity condition) is satisfied a priori. This necessary consistency condition is not satisfied if partial molar properties are computed via non-homogeneous operational definitions [9].

In what follows, we begin by outlining the methodology and presenting the appropriate operational definitions. We then discuss the transient behavior of the calculated properties. Finally, we illustrate the fluctuation method via a comparative study of the two asymmetric, binary Lennard-Jones mixtures. The complementary nature of the fluctuation and direct differentiation methods is addressed in the Conclusion section.

2. METHODOLOGY

The fluctuation method consists of two steps:

i) Derivation of an operational definition
ii) Simulation of the appropriate fluctuations

The operational definitions used here read

$$\bar{V}_j = \frac{V'}{<N>}\left[\sum_k x_k\,|\Delta|_{kj}\right]\left[\sum_k\sum_l x_k x_l |\Delta|_{kl}\right]^{-1} \tag{2}$$

$$\bar{U}_j = u\left[\sum_k x_k\,|\Delta|_{kj}\right]\left[\sum_k\sum_l x_k x_l |\Delta|_{kl}\right]^{-1} + \sum_i \langle \delta E \delta N_i \rangle \left[\frac{|\Delta|_{ij}}{|\Delta|} - \frac{(\sum_k x_k |\Delta|_{kj})\,(\sum_l x_l |\Delta|_{li})}{|\Delta| \sum_k \sum_l x_k x_l |\Delta|_{kl}}\right] \tag{3}$$

where x_i ($i = 1, \ldots, n$) is a mole fraction, $\langle\ \rangle$ denotes thermodynamic averaging within an open control volume V' containing, on average, $\langle N\rangle$ molecules, $|\Delta|_{ij}$ is the cofactor of the (i, j) element in the symmetric fluctuation determinant, $|\Delta|$, with elements

$$\Delta_{ij} = \langle \delta N_i \delta N_j \rangle = \langle N_i N_j \rangle - \langle N_i \rangle \langle N_j \rangle \tag{4}$$

and $\langle \delta E \delta N_i \rangle$ is the covariance of the instantaneous energy, E, and the number of molecules of species i, N_i. The specific energy u, is simply $\langle E\rangle / \langle N\rangle$, where $\langle E\rangle$ is the average energy of the control volume V'.

Equation (2) is the fluctuation-explicit Kirkwood-Buff expression [11] for the partial molar volume of the j^{th} component in a mixture ($j = 1, \ldots, n$). Equation (3) is derived in Appendix 1 (see also [10]). These expressions, together with the thermodynamic identity

$$\bar{H}_j = \bar{U}_j + P\bar{V}_j \tag{5}$$

relate the mechanical partial molar properties to concentration fluctuations and energy-concentration covariances within an open control volume. Equations (2) and (3) satisfy the homogeneity constraints

$$V' = \sum_i \langle N_i \rangle \bar{V}_i \tag{6}$$

$$\langle E \rangle = \sum_i \langle N_i \rangle \bar{U}_i \tag{7}$$

The implementation of the fluctuation expressions calls for the partitioning of the periodic box into a number of control volumes. Instantaneous compositions and energies within the control volumes are calculated at each time step, and the appropriate pairwise fluctuations, averaged over all control volumes, are then computed from the identity $\langle \delta x \delta y \rangle = \langle xy \rangle - \langle x \rangle \langle y \rangle$. Pairwise interaction energies are divided equally among the control volumes in which a given pair of molecules is located. If the control volumes are space-filling, it is also possible to partition configurational energies in proportion to the fraction of the pairwise separation vector lying within each region. The two recipes become indistinguishable in the thermodynamic limit. In this work, the former, computationally expendient approach was adopted (see below for consistency checks.)

The fluctuation-explicit operational definitions [Equations (2) and (3)] can be implemented via a variety of stochastic or deterministic methods. Here, we discuss (N, U, V) molecular dynamics. Use of space-filling control volumes then allows us to equate the specific energy and volume of Equations (2) and (3) to U/N and V/N, respectively, where N, V, and U are the total number of molecules, total volume, and total energy of the periodic box ($N = \sum \langle N \rangle_l$, $V = \sum V_l$, $U = \sum \langle E \rangle_l$; $l = 1, \ldots, L$; L = number of control volumes within the periodic box). Because of Equations (6) and (7), it is trivially true in (N, U, V) molecular dynamics with space-filling total energy of the periodic box ($N = \sum \langle N \rangle_l$, $V = \sum V'_l$, $U = \sum \langle E \rangle_l$; $l = 1, \ldots, L$; L = number of control volumes within the periodic box). Because of Equations (6) and (7), it is trivially true in (N, U, V) molecular dynamics with space-filling control volumes that $U = \sum N_i \bar{U}_i$, and $V = \sum N_i \bar{V}_i$ (Euler's homogeneous function theorem). The same is true for the mixture enthalpy, with the important difference, however, that the latter is a fluctuating quantity in any constant volume simulation.

The distinguishing feature of the fluctuation approach is that the partial molar properties of all species are obtained simultaneously, and the calculations are independent of the number of components in the mixture. The equation $\lambda = \sum N_i\bar{\lambda}_i$ (Euler's theorem, a necessary consistency condition), is satisfied identically. In addition, the following independent consistency tests have been performed [9, 10]:

(i) The operational definitions were applied to a "trivial" Lennard-Jones mixture. A "trivial" mixture is a one-component system in which molecules differ only by virtue of their labels (for example, N_1 "solute" and N–N_1 "solvent" molecules with identical interaction potentials). In such a mixture, $\bar{U}_i = U/N$ and $\bar{V}_i = V/N$, and the partial molar quantities are therefore known a priori. Application of Equations (2) and (3) gives rise to numbers that can be compared to the exact values. For $N = 256$ and $N_1 = 3, 26, 38, 51$, and 77, percent absolute errors in energy and volume were, respectively, (15.3, 13.4), (2.8, 0.4), (3.1, 1.3), (4.8, 2.1), (2.3, 2.3), for the "solute", and (0.2, 0.2), (0.3, 0.1), (0.5, 0.2), (1.2, 0.5), (1.0, 1.0), for the "solvent".

(ii) The sample size dependence was tested by increasing N from 256 to 500 (and N_1 correspondingly, from 77 to 150) for an asymmetric binary Lennard-Jones mixture in which $\varepsilon_1/\varepsilon_2 = .597$, and $\sigma_1/\sigma_2 = .768$, at $kT/\varepsilon_2 = 0.93 \pm 0.03$ and $N\sigma_2^3/V = 0.8594$. The computed partial molar properties changed by less than 5%.

(iii) The number of control volumes was doubled in the course of two otherwise identical "trivial" mixture simulations, at $kT/\varepsilon = 0.974 \pm 0.03$ and $N\sigma^3/V = 0.8594$. The computed partial molar properties changed by less than 2.5%.

3. TRANSIENT BEHAVIOR

The most important numerical question assoicated with the method's implementation is the relaxation time required for the calculation of fluctuations. We first introduce the following notation ($i = 1, 2$; $1 =$ solute, $2 =$ solvent)

$$\bar{V}_i^* = \bar{V}_i/\sigma_2^3 \qquad t^* = t/(l\sqrt{m_1/\varepsilon_2})$$

$$\bar{U}_i^* = \bar{U}_i/\varepsilon_2 \qquad P^* = P\sigma_2^3/\varepsilon_2$$

$$U^* = U/\varepsilon_2 \qquad m_i^* = m_i/m_1$$

$$\varrho^* = N\sigma_2^3/l^3 = 6\phi/\pi \qquad T^* = kT/\varepsilon_2$$

where l is the length of the periodic box, t denotes time, m, mass, and ϕ, volume fraction.

Figure 1 shows the time-dependent behavior of the solute's partial molar volume over four different (N, U, V) molecular dynamics simulations of binary Lennard-Jones mixtures having N_1 solute and (256-N_1) solvent molecules, with $\sigma_1/\sigma_2 = .768$, $\varepsilon_1/\varepsilon_2 = .597$, $l/\sigma_2 = 6.6784$, $m_2/m_1 = 1.318$, and Lorentz-Berthelot combining rules. The average temperature corresponding to $N_1 = 3, 26, 85, 90$, was .938 (± .03), .939 (± .03), .921 (± .02), and .916 (± .02), respectively. Technical details pertaining to all simulations discussed in the paper are included in Appendix 2.

After a relaxation time $t^* \approx 10$, $\bar{V}_1^*$ is always within 6% of its final value. For the integration steps used in Figure 1, this corresponds to a number of steps ranging from 22000 ($N_1 = 90$) to 37000 ($N_1 = 3$). As expected, the magnitude of initial fluctuations in $\bar{V}_1^*$ decreases as N_1 increases. Since the calculation of $\bar{V}_i$ involves only concentration fluctuations (i.e., counting molecules within a control volume), the relaxation behavior shown in Figure 1 is indicative of the time required for molecules

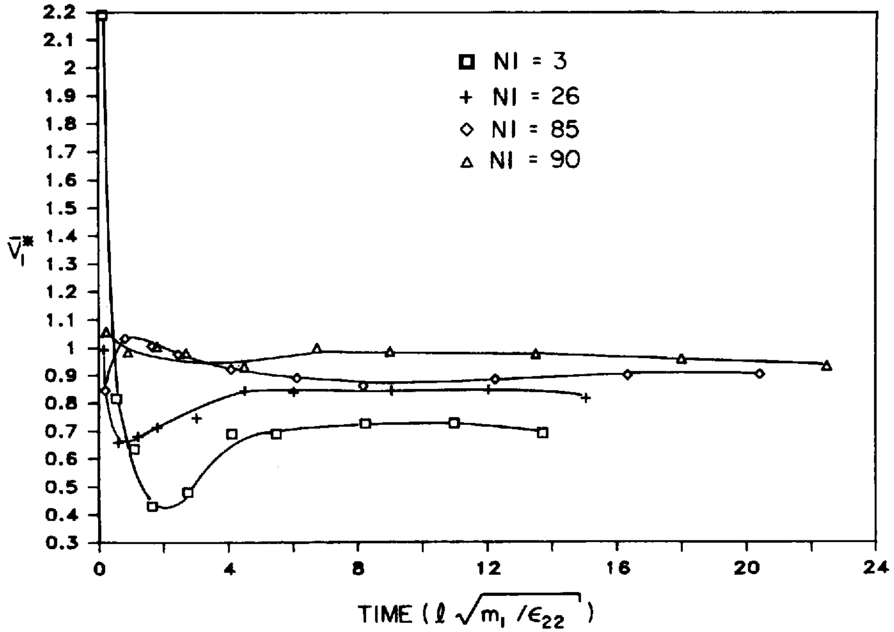

Figure 1 Transient behavior of the calculated solute partial molar volume. Mixture 1 (Runs 1, 2, 7, 8).

to mix, and to sample control volumes adequately. The latter time should, in principle, be related to the time needed for the system to lose memory of a given spatial configuration. The configurational relaxation can be conveniently represented in graphical form in a way originally proposed by Panagiotopoulos [12]. Figures 2 and 3 show the coordinates of 256 identical Lennard-Jones atoms [$\varrho^* = 0.8594$, $T^* = 0.974$ ($\pm$ 0.03)] at different times, plotted against the coordinates at an arbitrarily chosen "initial" time, and exhibit behavior typical of the systems studied in this work. After 6000 time steps, $t^* = 2.71$ ($\Delta t^* = 4.52 \times 10^{-4}$). This means that the relaxation time for concentration fluctuations (Figure 1) is of the order of 3 spatial configuration memory losses, which suggests that inter-species mixing is a slower process than spatial relaxation.

Note that the fluctuation-based calculation of partial molar energies [Equation (3)] involves energy-concentration covariances in addition to pure concentration fluctuations. The time-dependent behavior of the former is illustrated in Figure 4 for a binary Lennard-Jonesium of 128 solute and 128 solvent molecules, with $\varepsilon_1/\varepsilon_2 = 1$, $\sigma_1/\sigma_2 = .768$, $m_2/m_1 = 1.318$, and Lorentz-Berthelot combining rules. The density and temperature corresponding to this simulation are $\varrho^* = 0.8594$, $T^* = 1.128$ ($\pm$ 0.03). Figure 5 shows the time-dependent behavior of concentration fluctuations for a $N_1 = 85$ binary Lennard-Jonesium (Figure 5 and the $N_1 = 85$ curve in Figure 1 correspond to identical simulations).

In general, then, the calculation of mechanical partial molar properties via the simulation of the appropriate fluctuations involves relaxation times of the order of a few spatial configuration relaxations. This time corresponds to an adequate sampling of the control volumes within which fluctuations are computed.

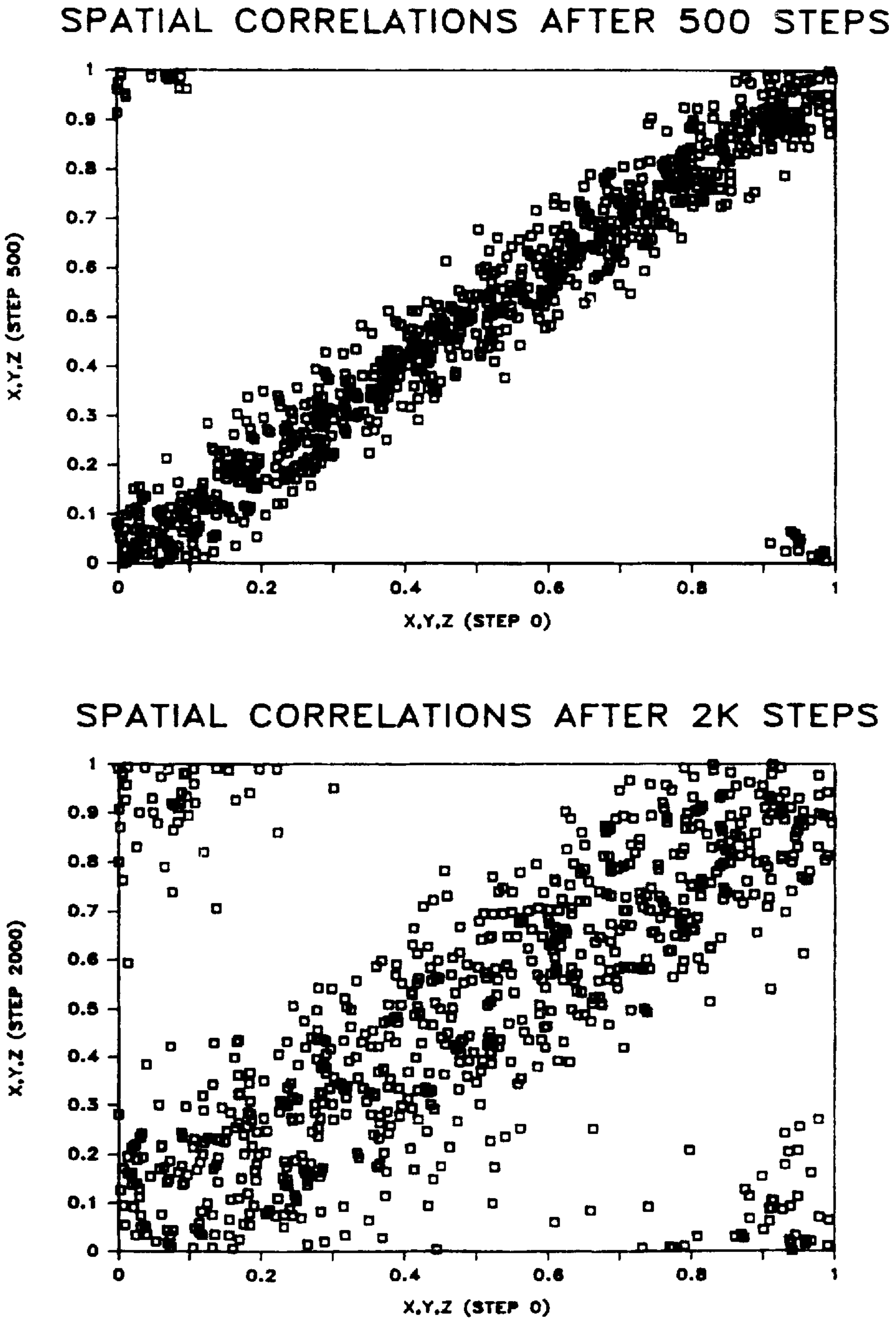

Figure 2 Coordinates of 256 identical Lennard-Jones atoms at successive times plotted against the corresponding values at an arbitrarily chosen "initial" time. $T^* \approx 0.97(3)$; $\rho^* = 0.8594$.

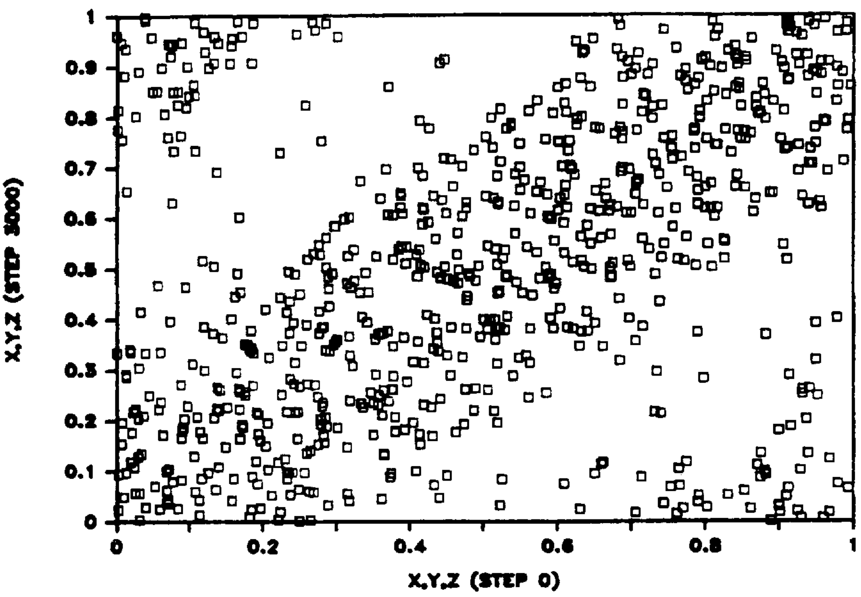
SPATIAL CORRELATIONS AFTER 3K STEPS

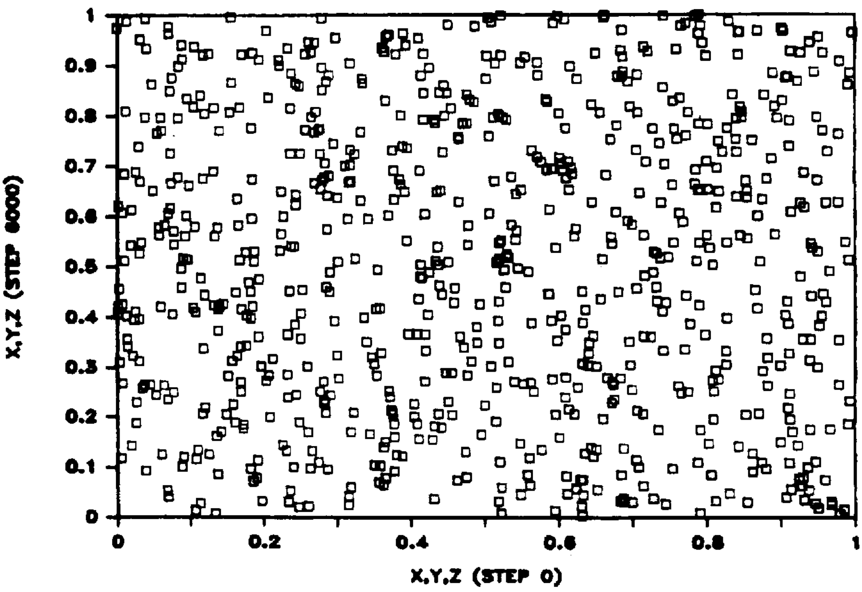
SPATIAL CORRELATIONS AFTER 6K STEPS

Figure 3 Coordinates of 256 identical Lennard-Jones atoms at successive times plotted against the corresponding values at an arbitrarily chosen "initial" time. $T^* = 0.97(3)$; $\varrho^* = 0.8594$.

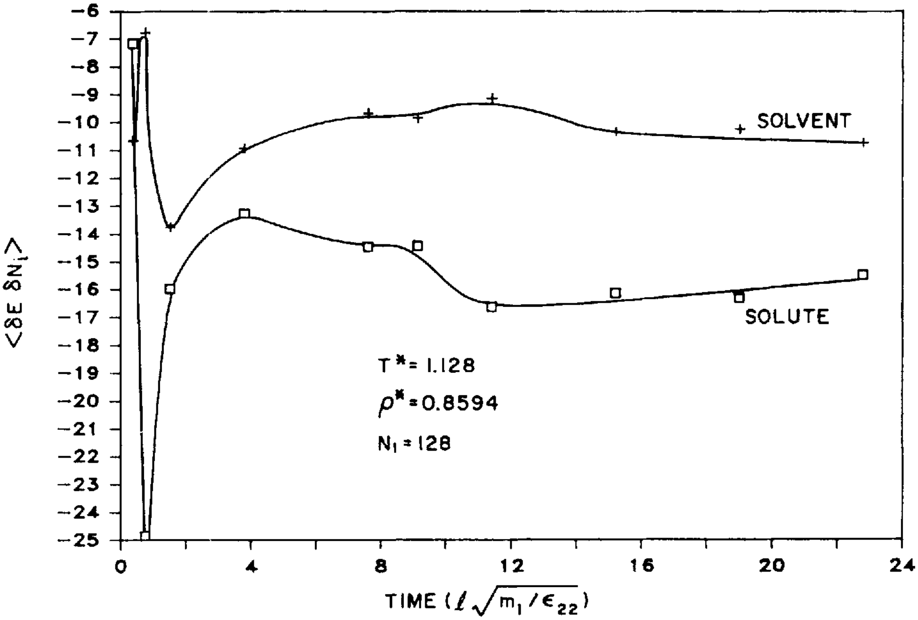

Figure 4 Transient behavior of calculated correlations between energy and component molelule number fluctuations (per control volume). Mixture II (Run 12).

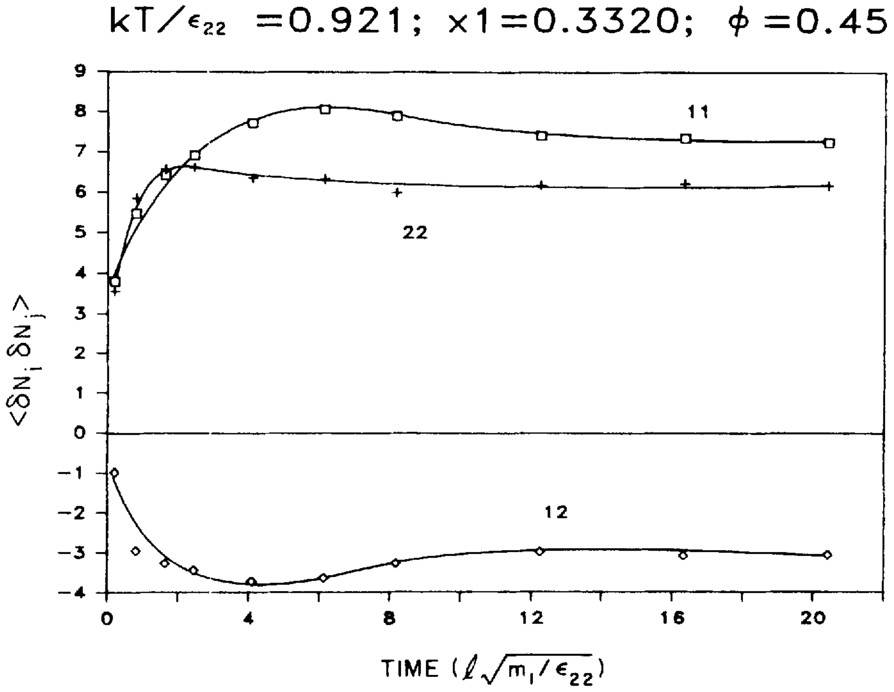

Figure 5 Transient behavior of calculated pairwise concentration fluctuations (per control volume). Mixture I (Run 7).

4. RESULTS

Two asymmetric Lennard-Jones mixtures with shifted force potentials [13] were studied in this work. They are described in Table 1. Phase coexistence boundaries for these mixtures have been previously obtained [14] via (N, V, T) Monte Carlo simulations. All of the simulations performed performed here were in the single phase region. The specific studies performed are listed in Table 2. Simulation results are shown in Table 3.

Enthalpy calculations (Table 3) have significantly larger uncertainties than the corresponding volume and energy numbers. This is a consequence of the fact that pressure is a fluctuating quantity in any constant volume simulation [see Equation (A2–3) and Table A2.1], and implies that quantitative accuracy in enthalpy calculations calls for isobaric simulations. Fluctuation-based operational definitions for partial molar enthalpy calculations at finite concentrations in isobaric simulations have been recently derived [15].

The first eight runs in Table 3 correspond to an isothermal composition change at constant total number density. The nominal volume fraction based on the solvent's Lennard-Jones diameter is given by $\phi = \pi\varrho^*/6$. The effective volume fraction $\phi_{\text{eff}} = \phi[(1 - x_1) + x_1(\sigma_1/\sigma_2)^3]$ decreases from 0.447 to 0.363 as x_1 increases from 1.17% to 35.16%, since solute molecules are smaller than solvent molecules. This gives rise to a pressure decrease, as shown in Table 3. The composition dependence of the mechanical partial molar quantities is shown in Figures 6–8. In all cases, the homogeneity constraint is satisfied identically (this is true for any simulation result but not necessarily for the number quoted in Table 3, where results have been rounded to the last significant digit and the corresponding uncertainty has been included in parenthesis). If we assign a volume $\pi\sigma_i^3/6$ to molecules, then each solute molecule contributes 2.9 times its size to the total volume when the mixture composition is 1.17% solute, and 3.92 times its size for $x_1 = 35.16\%$. The solvent, on the other hand, expands from 2.23 to 2.46 times its size when the mixture is expanded by increasing the solute mole fraction at constant total number density. The slope in the enthalpy curves reflects the fact that pressure decreases as the solute concentration increases. For a temperature $T^* = 0.94$, the kinetic energy per molecule is equal to 1.41 solvent

Table 1 Mixtures Studied in this Work[(a)]

	σ_1/σ_2	$\varepsilon_1/\varepsilon_2$	m_2/m_1
Mixture I	.768	.597	1.318
Mixture II	.768	1.000	1.318

(a) Lorentz-Berthelot combining rules were used to obtain σ_{12} and ε_{12}.

Table 2 Numerical Studies Performed in this Work[(a)]

Study (b)	*Mixture*	N_1	ϱ^*
1 (runs 1–8)	I	$3 \leqslant N_1 \leqslant 90$	0.8594
2 (runs 9–12)	II	$15 \leqslant N_1 \leqslant 128$	0.8594

(a) Average temperatures for studies 1 and 2, were 0.93 and 1.16, respectively (see Table 3).
(b) See Table 3.

Table 3 Simulation Results[(a)]

Simulation	N_1	ϱ^*	U^*/N	T^*	P^*	$\bar{V}_1^*$	$\bar{V}_2^*$	$\bar{U}_1^*$	$\bar{U}_2^*$	$\bar{H}_1^*$	$\bar{H}_2^*$
1	3	.8594	−3.3894(2)	0.94(3)	2.52(±.2)	0.69(2)	1.1691(2)	−1.0(1)	−3.418(1)	0.75(±.29)	−0.47(±.24)
2	26	.8594	−3.0418(3)	0.94(3)	1.82(±.21)	0.82(1)	1.203(1)	−1.17(9)	−3.25(2)	0.32(±.27)	−1.06(±.26)
3(b)	38	.8594	−2.9063(9)	0.91(3)	1.47(±.2)	0.83	1.222	−1.25	−3.195	−0.032	−1.40
4(b)	51	.8594	−2.6654(8)	0.93(3)	1.27(±.2)	0.85	1.242	−1.12	−3.050	−0.037	−1.47
5(b)	64	.8594	−2.4770(4)	0.93(3)	1.05(±.2)	0.90	1.250	−1.101	−2.965	−0.065	−1.65
6(b)	77	.8594	−2.2966(8)	0.92(3)	0.84(±.21)	0.88	1.287	−0.97	−2.867	−0.23	−1.78
7	85	.8594	−2.1865(4)	0.92(3)	0.71(±.2)	0.90(2)	1.292(8)	−0.88(4)	−2.84(2)	−0.24(±.24)	−1.92(±.29)
8	90	.8594	−2.1234(5)	0.92(2)	0.65(±.2)	0.93(2)	1.29(1)	−0.82(2)	−2.83(1)	−0.21(±.21)	−1.99(±.28)
9	15	.8594	−2.809(1)	1.15(4)	3.23(±.24)	0.723(2)	1.191(2)	−2.13(9)	−2.851(5)	0.20(±.27)	0.99(±.29)
10	64	.8594	−2.3419(6)	1.19(3)	1.88(±.25)	0.855(6)	1.267(5)	−1.94(6)	−2.48(2)	−0.33(±.29)	−0.09(±.35)
11	96	.8594	−2.1594(6)	1.15(3)	1.06(±.25)	0.849(2)	1.352(1)	−1.83(2)	−2.35(5)	−0.94(±.23)	−0.93(±.38)
12	128	.8594	−1.9290(6)	1.13(3)	0.55(±.24)	0.902(6)	1.426(9)	−1.68(3)	−2.18(3)	−1.19(±.25)	−1.40(±.37)

(a) The notation 1.203(1) denotes 1.203 ± 0.001.
(b) $\bar{V}_i$, $\bar{U}_i$ and $\bar{H}_i$ values for these runs were computed only once, at the end of the simulation.

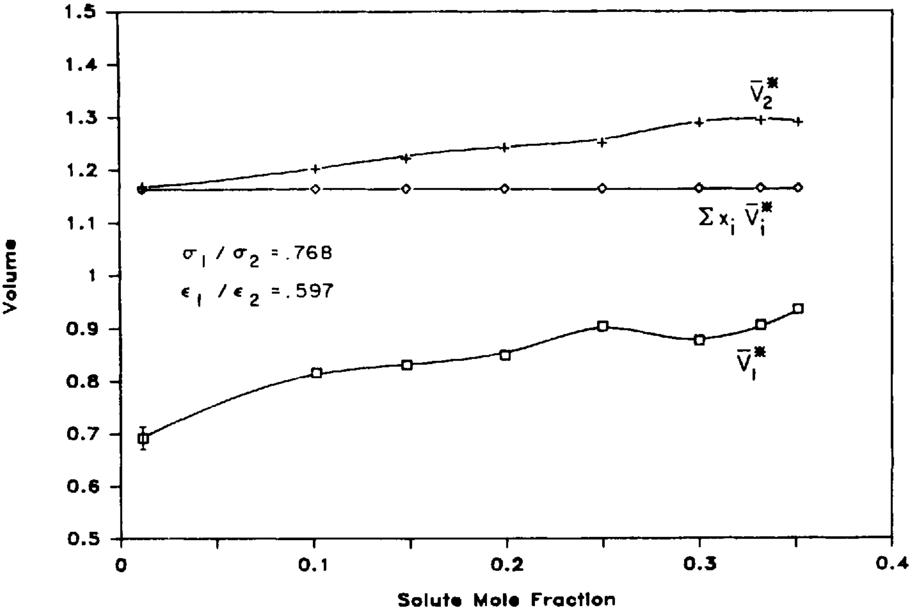

Figure 6 Composition dependence of partial molar volumes at constant temperature and number density. Mixture I (Runs 1–8); $T^* \approx 0.93$, $\varrho^* = 0.8594$. Only maximum error bar shown.

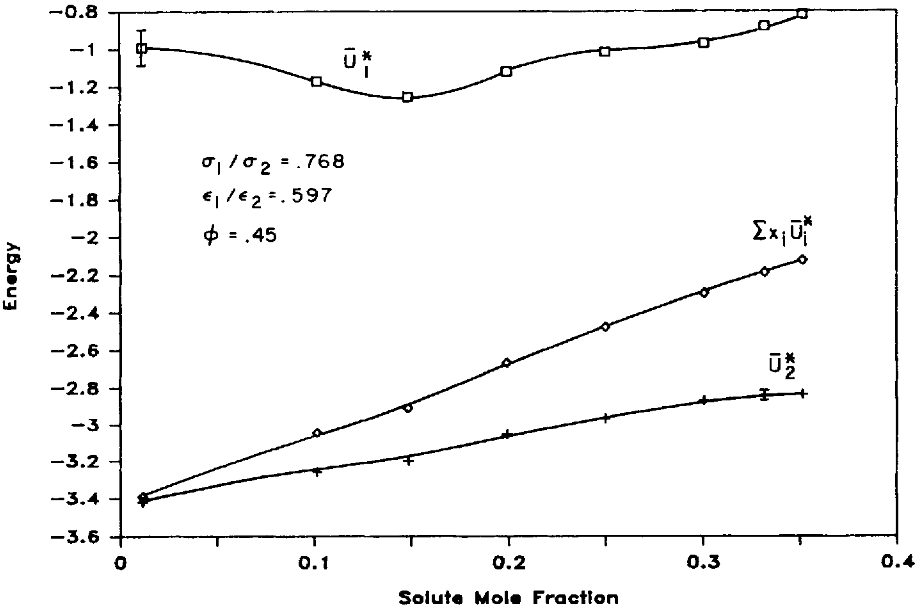

Figure 7 Composition dependence of partial molar energies at constant temperature and number density. Mixture I (Runs 1–8); $T^* \approx 0.93$, $\varrho^* = 0.8594$. Maximum error bars shown.

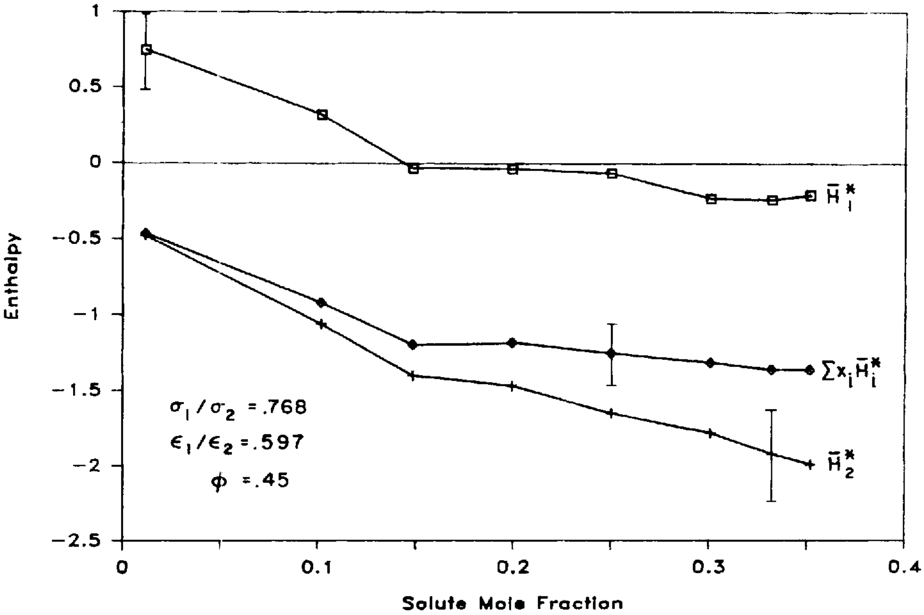

Figure 8 Composition dependence of partial molar enthalpies at constant temperature and number density. Mixture I (Runs 1–8): $T^* \approx 0.93$, $\varrho^* = 0.8594$. Maximum error bars shown.

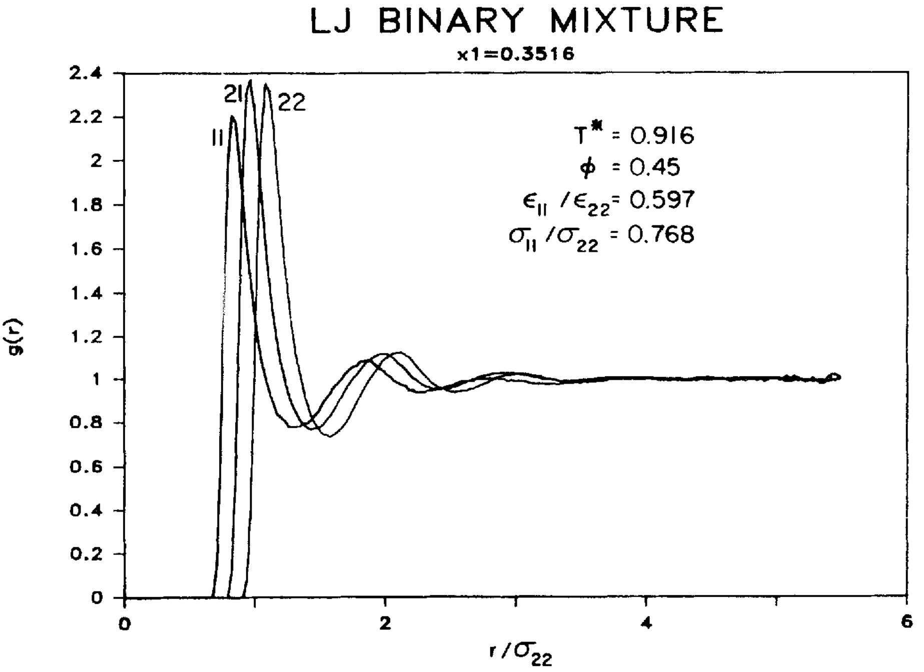

Figure 9 Pair correlation functions for Mixture I (Run 8).

well depths. Thus, the solute's configurational energy (or, more appropriately, the configurational contribution to its partial molar energy) is roughly 2.4 solvent well depths; for the solvent, this number varies from 4.8 ($x_1 = 1.17\%$) to 4.2. The ratio of ocnfigurational contributions to the respective partial molar energies is thus very similar to the ratio of well depths. The mixture structure is shown in Figure 9. The method of Theodorou and Suter [16] has been used to extend the computation of $g(r)$ beyond 0.51 (or, equivalently, beyond $3.34\sigma_2$).

Runs 9–12 (Table 3) correspond to an isothermal composition change at constant total number density, applied this time to mixture II, which is asymmetric in size but symmetric in energy. As before, increasing the solute mole fraction leads to a pressure decrease. The composition dependence of the mechanical partial molar quantities is shown in Figures 10–12. Upon expanding the mixture from $\phi_{\text{eff}} = 0.4356$ ($x_1 = 5.86\%$) to $\phi_{\text{eff}} = 0.3269$ ($x_1 = 50\%$) the solute's partial molar volume changes from 3.05 to 3.8 times its size; the solvent's partial molar volume, from 2.28 to 2.72 times its size. This behavior is very similar to the one exhibited by mixture I, indicating, in this case, that energetic contributions to the partial molar volume are of secondary importance when compared to purely geometric factors, such as the size difference between solute and solvent. At a temperature $T^* = 1.15$, the kinetic energy per molecule is 1.725 well depths. The solute's configurational contribution to its partial molar energy decreases from 3.86 to 3.41 well depths as ϕ_{eff} is reduced from 43.56% to 32.69% by replacing solvent by solute molecules at constant number density. For the solvent, the corresponding decrease is from 4.58 to 3.90 well depths. Comparison with mixture I shows that changing ε_1 from 0.597 to 1 solvent well depths has a profound effect on the configurational contribution to $\bar{U}_1$, and a moderate effect

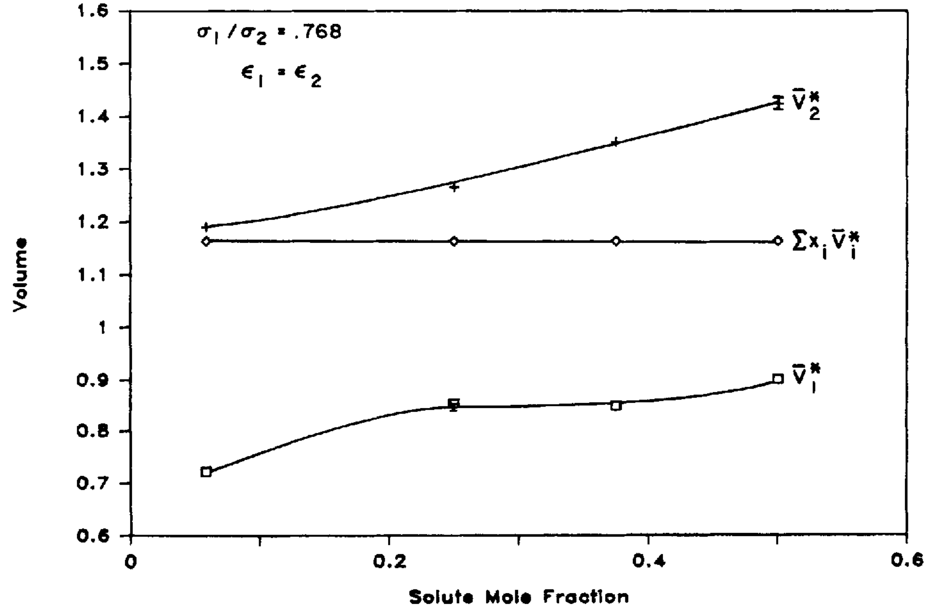

Figure 10 Composition dependence of partial molar volumes at constant temperature and number density. Mixture II (Runs 9–12); $T^* \approx 1.15$, $\varrho^* = 0.8594$. Maximum error bars shown.

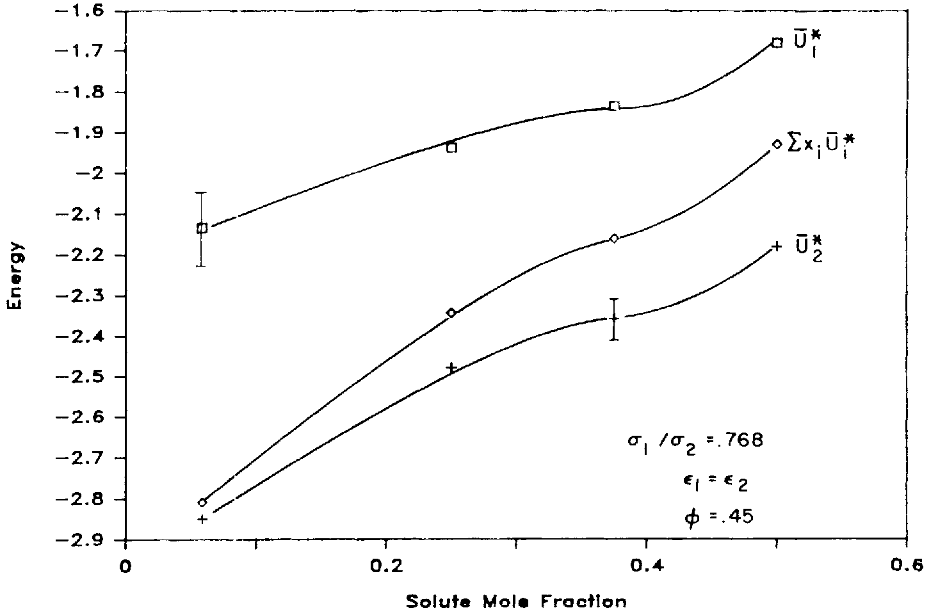

Figure 11 Composition dependence of partial molar energies at constant temperature and number density. Mixture II (Runs 9–12): $T^* \approx 1.15$, $\varrho^* = 0.8594$. Maximum error bars shown.

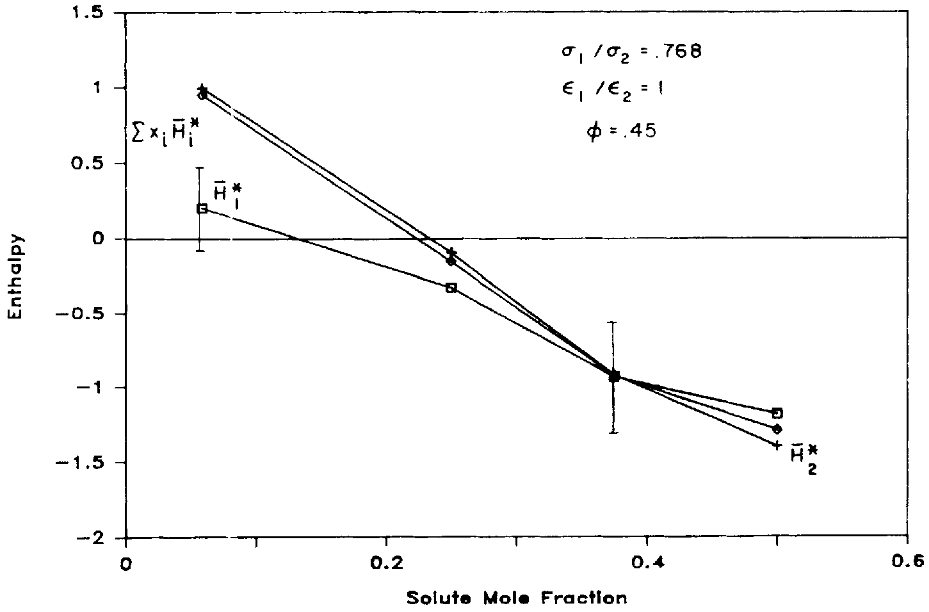

Figure 12 Composition dependence of partial molar enthalpies at constant temperature and number density. Mixture II (Runs 9–12); $T^* \approx 1.15$, $\varrho^* = 0.8594$. Maximum error bars shown.

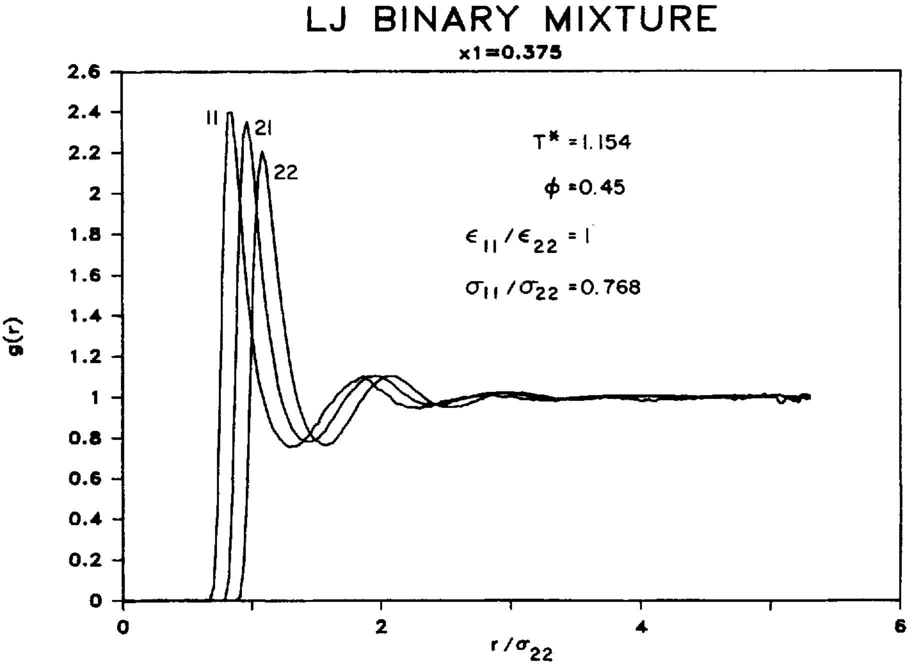

Figure 13 Pair correlation functions for Mixture II (Run 11).

on $\bar{U}_2$. Because solvent and solute molecules now have identical well depths, differences between their configurational partial molar energies are entirely due to size asymmetry. At high volume fraction (low x_1), this configurational energy difference is 0.72 well depths, and it decreases to 0.5 well depths when x_1 is 50%. This represents roughly 15% of the respective configurational contributions to the partial molar energies. The mixture structure is shown in Figures 13 and 14. The former, when compared with Figure 9, shows the effect of increasing the solute's characteristic energy from 0.597 to 1 solvent well depths (the effective volume fractions in Figures 9 and 13 are 0.363 and 0.358, respectively; note however, the different temperatures). The first peak in the solute-solute pair correlation functions increases from 2.21 to 2.40; the solvent-solvent peak is reduced from 2.36 to 2.21. Comparison of Figures 13 and 14, on the other hand, shows the effect of diluting the mixture at constant number density and temperature. Because of the size difference between solute and solvent, this leads to an increase in the effective volume fraction from 0.358 ($x_1 = 37.5\%$) to 0.436 ($x_1 = 5.86\%$). The ordering arising as a result of this 21.8% increase in the effective volume fraction can be seen from the growth in the secondary solvent-solvent and solute-solvent peaks, from 1.10 to 1.22, and from 1.11 to 1.21, respectively, and from the existence of correlations ($g \neq 1$) over distances greater than 0.51 (i.e., $3.34\sigma_2$).

It is interesting to compare the above discussed simulation results with theoretical calculations. The recently published version of perturbation theory due to Shukla [17] has been shown to provide reliable values for a variety of thermodynamic properties of binary mixtures of atomic fluids (including excess volumes, enthalpies, Gibbs and

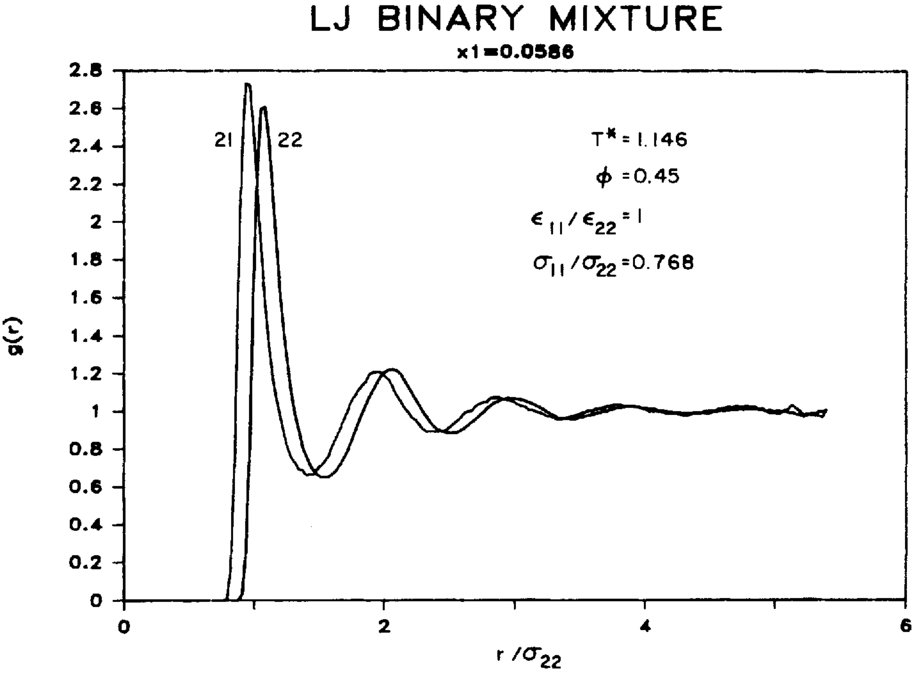

Figure 14 Pair correlation functions for Mixture II (Run 9).

Helmholtz energies, as well as chemical potentials), over a wide range of size and energy parameter ratios. The key idea behind this theory is the evaluation of hard-sphere diameters in such a way as to eliminate the first order correction to the reference residual free energy [17]. The author is grateful to one of the paper's referees, who used molecular parameters as per Table 1 to calculate the Shukla perturbation theory values for the mechanical partial molar properties of the model shifted Lennard-Jones mixtures under study. It should be emphasized, however, that this comparison is based on T^* and P^*, both of which (but especially the latter) fluctuate in (N, U, V) simulations (see Table A2.1).

For mixture I (runs 1–8), these calculations yielded average, average absolute, and maximum percent differences (with respect to simulation values) of [-15.61, 15.61, and -19.5 ($\bar{V}_1^*$)], [2.44, 2.44, and 3.88 ($\bar{V}_2^*$)] [2.34, 12.69, and -38 ($\bar{U}_1^*$)], and [-3, 3.28 and -6.03 ($\bar{U}_2^*$)]. Not surprisingly, maximum differences correspond to runs 1 and 2 ($x_1 \leqslant 10.1\%$). If we consider only simulations for which $x_1 \geqslant 15\%$ (runs 3–8), the corresponding maximum percent differences become -18.9 ($\bar{V}_1^*$) and 14.62 ($\bar{U}_1^*$).

In the case of mixture II (runs 9–12), which is only asymmetric with respect to the size parameters, the calculations yielded average, average absolute, and maximum percent differences (with respect to the simulation results) of [-22.03, 22.03, and -25.15 ($\bar{V}_1^*$)], [5.08, 5.08, and 5.77 ($\bar{V}_2^*$)], [-32.64, 32.64, and -37.08 ($\bar{U}_1^*$)], and [7.45, 7.45, and 15.14 ($\bar{U}_2^*$)]. Since the fluctuation method is based upon an adequate sampling of control volumes, it seems plausible to attribute these systematic differences for mixture II to increased solute-solute association (and hence decrease in mobility), as shown by the already mentioned increase in the first peak of g_{11}.

5. CONCLUSIONS

Equations (2) and (3) are fluctuation-explicit operational definitions of the partial molar volume and energy of a component in a mixture. Both relationships were derived invoking the formalism of the grand canonical ensemble [10, 11]. Equations (2) and (3) satisfy Euler's homogeneous function theorem identically (i.e., $U = \sum \bar{U}_i N_i$, $V = \sum \bar{V}_i N_i$) and can be used as a basis for the computer calculation of mechanical partial molar properties.

The advantages and limitations of the fluctuation method for the computer calculation of mechanical partial molar properties are, interestingly, complementary to those associated with the direct differentiation approach. The fluctuation method allows the simultaneous calculation of the properties of interest for all components in the mixture. The simulation's length is completely independent of the number of components in the mixture. By contrast, in direct differentiation methods, one particle addition/removal experiment per component is required. (In the specific case of binary mixtures, however, simultaneous information on both components can, in principle, be obtained by applying the tangent-intercept rule [8] to a numerical fit of the composition dependence of the corresponding extensive property over a series of isothermal-isobaric simulations, but this approach calls for a large number of intermediate simulations to obtain accurate partial molar properties). The fluctuation method is ideally suited for the calculation of properties in mixtures where all component mole fractions are higher than (approximately) 15%. The isothermal-isobaric particle removal/addition which characterizes the direct differentiation method, on the other hand, is ideally suited for the simulation of infinitely dilute mixtures, provided the same pressure is used to simulate both the pure solvent and the solvent with a single solute molecule. This procedure is clearly approximate away from infinite dilution. Although no results from (N, P, T) direct differentiation simulations at finite concentrations are available in the literature, comparisons with perturbation theory [17] show maximum percent differences of 19% ($\bar{V}_1^*$) and 15% ($\bar{U}_1^*$) for mixture I ($x_1 \geqslant 15\%$), and 25% ($\bar{V}_1^*$) and 37% ($\bar{U}_1^*$) for mixture II.

The fluctuation method, though appropriate for finite concentrations, requires considerably longer simulations, since the appropriate time scale relevant to the calculation of a fluctuation, namely, a configurational memory loss, exceeds the characteristic times required to calculate the corresponding "primitive" properties [i.e., $t(\langle x \rangle) \sim t(\langle y \rangle) < t(\langle xy \rangle - \langle x \rangle \langle y \rangle)$]. The meaningful comparison, however, is between a fluctuation simulation and the number of direct differentiation simulations required to obtain the same information (three for a binary mixture; more than this number if interpolation and the tangent-intercept rule are used). It is clear that the fluctuation method becomes more advantageous the greater the number of components in the mixture under study.

Application of the fluctuation method to the study of two asymmetric model mixtures resulted in an individualization of distinct size and energy contributions to a mixture's mechanical partial molar properties at finite species concentrations. Systematically planned computer "experiments" such as these can lead to a significant improvement in our current understanding of the molecular basis underlying the thermal and volumetric properties of mixtures. The (N, U, V) molecular dynamics implementation of the fluctuation-explicit operational definitions by no means exhausts the method's possibilities: stochastic and deterministic simulations in which thermodynamic observables (such as temperature and pressure) are imposed upon the mixture under study represent obvious extensions. This is especially important in the case of enthalpy calculations, where the pressure fluctuations which characterize (N, U, V) simulations (see Table A2.1) give rise to large uncertainties in the value of the computed properties (see Table 3). Fluctuation-based operational definitions which specifically address this problem are discussed elsewhere [15].

Acknowledgement

All calculations were performed on a Cyber 205 machine at the John von Neumann Center for Scientific Computing at Princeton. Supercomputer time grants from the National Science Foundation (CBT-8517739) and the John von Neumann Center National Allocations Committee, and the financial support of the National Science Foundation (grant CBT-8657010) are gratefully acknowledged.

APPENDIX 1

We first express differential energy changes in terms of the independent variables appropriate to the grand canonical ensemble ($\beta = 1/kT$)

$$dU = \left(\frac{\partial U}{\partial V}\right)_{\beta,\{\beta\mu\}} dV + \left(\frac{\partial U}{\partial \beta}\right)_{V,\{\beta\mu\}} d\beta + \sum_{\mathrm{i}} \left(\frac{\partial U}{\partial \beta\mu_{\mathrm{i}}}\right)_{\beta,V,\beta\mu[i]} d\beta\mu_{\mathrm{i}} \tag{A1-1}$$

where the notation $\{\beta\mu\}$ denotes constancy of all μ_{j}/T, and $\beta\mu$[i], constancy of all μ_{j}/T except for μ_{i}/T. Application of Euler's honogeneous function theorem yields

$$\left(\frac{\partial U}{\partial V}\right)_{\beta,\{\beta\mu\}} = \frac{U}{V} \tag{A1-2}$$

and, therefore,

$$\bar{U}_{\mathrm{j}} = \left(\frac{U}{V}\right) \bar{\mathrm{V}}_{\mathrm{j}} + \sum_{\mathrm{i}} \langle \delta E \delta N_{\mathrm{i}} \rangle \left(\frac{\partial \beta\mu_{\mathrm{i}}}{\partial \mathrm{N}_{\mathrm{j}}}\right)_{T,P,N[j]} \tag{A1-3}$$

where we distinguish E, the instantaneous energy of a member of the grand canonical ensemble from U, its average (thermodynamic) energy (i.e., $U = \langle E \rangle$), and we have used the identity [10]

$$\left(\frac{\partial U}{\partial \beta\mu_{\mathrm{i}}}\right)_{\beta,V,\beta\mu[i]} = \langle \delta E \delta N_{\mathrm{i}} \rangle \tag{A1-4}$$

Both the partial molar volume and the chemical potential derivative in Equation (A1-3) can be written in terms of concentration fluctuations through the well known Kirkwood-Buff expressions [11]

$$\bar{V}_{\mathrm{j}} = \mathrm{v}\left[\sum_{\mathrm{k}} x_{\mathrm{k}} |\Delta|_{\mathrm{kj}}\right]\left[\sum_{\mathrm{k}} \sum_{\mathrm{l}} x_{\mathrm{k}} x_{\mathrm{l}}\, |\Delta|_{\mathrm{kl}}\right]^{-1} \tag{A1-5}$$

$$\beta\left(\frac{\partial \mu_{\mathrm{i}}}{\partial N_{\mathrm{j}}}\right)_{\beta,\mathrm{P},\mathrm{N[j]}} = \frac{|\Delta|_{\mathrm{ij}}}{|\Delta|} - \left(\sum_{\mathrm{k}} x_{\mathrm{k}}\, |\Delta|_{\mathrm{kj}}\right)\left(\sum_{\mathrm{l}} x_{\mathrm{l}}\, |\Delta|_{\mathrm{li}}\right)\left[|\Delta| \sum_{\mathrm{k}} \sum_{\mathrm{l}} x_{\mathrm{k}} x_{\mathrm{l}}\, |\Delta|_{\mathrm{kl}}\right]^{-1} \tag{A1-6}$$

Substitution of Equations (A1-5) and (A1-6) into (A1-3) yields the desired result ($u = U\langle N \rangle^{-1}$)

$$\bar{U}_j = \frac{u\sum_k x_k|\Delta|_{kj}}{\sum_k\sum_l x_k x_l|\Delta|_{kl}} + \sum_i \langle \delta E \delta N_i \rangle \times \left[\frac{|\Delta|_{ij}}{|\Delta|} - \frac{\left(\sum_k x_k|\Delta|_{kj}\right)\left(\sum_l x_l|\Delta|_{li}\right)}{|\Delta|\left(\sum_k\sum_l x_k x_l|\Delta|_{lk}\right)}\right] \tag{A1-7}$$

For a binary mixture, this expression reads

$$\bar{U}_1 = \frac{u[x_1\langle(\delta N_2)^2\rangle - (1-x_1)\langle\delta N_1\delta N_2\rangle]}{x_1^2\langle(\delta N_2)^2\rangle - 2x_1(1-x_1)\langle\delta N_1\delta N_2\rangle + (1-x_1)^2\langle(\delta N_1)^2\rangle} + \frac{(1-x_1)^2\langle\delta E\delta N_1\rangle - x_1(1-x_1)\langle\delta E\delta N_2\rangle}{x_1^2\langle(\delta N_2)^2\rangle - 2x_1(1-x_1)\langle\delta N_1\delta N_2\rangle + (1-x_1)^2\langle(\delta N_1)^2\rangle} \tag{A1-8}$$

APPENDIX 2

The equations of motion were integrated via a Verlet scheme [18]

$$\mathbf{r}(t+\Delta t) = 2\mathbf{r}(t) - \mathbf{r}(t-\Delta t) + \frac{\mathbf{F}(t)}{m}\Delta t^2 + 0(\Delta t^4) \tag{A2-1}$$

where $\mathbf{r}$ is the particle position, m, its mass, and $\mathbf{F}$, the force on the particle. A shifted potential [13], with cutoff at $r_c = 2.8\,\sigma_2$ was used throughout. Time steps (Δt) used in the various simulations, as well as energy conservation, run duration, temperature and pressure fluctuations, are listed in Table A2.1. In a Verlet algorithm, velocities (which are not used in the integration of the equations of motion) are obtained from the approximation

$$\dot{\mathbf{r}}(t) = [\mathbf{r}(t+\Delta t) - \mathbf{r}(t-\Delta t)]/(2\Delta t) + 0(\Delta t^2) \tag{A2-2}$$

Table A2.1 Time Steps, Run Durations, Energy Conservation

Run	$10^4\Delta t^*$	$\langle(\delta U)^2\rangle^{1/2}/\lvert\langle U\rangle\rvert$	$\langle(\delta T)^2\rangle^{1/2}/\langle T\rangle$	$\langle(\delta P)^2\rangle^{1/2}/\langle P\rangle$	*Duration (steps)*
1	2.74	6.14×10^{-5}	3.20×10^{-2}	7.95×10^{-2}	50000
2	3.01	1.04×10^{-4}	3.14×10^{-2}	1.17×10^{-1}	50000
3	13.25	2.95×10^{-4}	3.06×10^{-2}	1.40×10^{-1}	30000
4	6.35	3.05×10^{-4}	3.03×10^{-2}	1.61×10^{-1}	40000
5	6.77	1.73×10^{-4}	2.88×10^{-2}	1.93×10^{-1}	30000
6	7.82	3.39×10^{-4}	2.87×10^{-2}	2.47×10^{-1}	30000
7	4.08	1.77×10^{-4}	2.79×10^{-2}	2.83×10^{-1}	50000
8	4.50	2.45×10^{-4}	2.76×10^{-2}	3.06×10^{-1}	50000
9	3.41	3.74×10^{-4}	3.13×10^{-2}	7.40×10^{-2}	30000
10	5.33	2.47×10^{-4}	2.93×10^{-2}	1.34×10^{-1}	30000
11	6.65	2.96×10^{-4}	2.72×10^{-2}	2.34×10^{-1}	30000
12	7.60	2.90×10^{-4}	2.66×10^{-2}	4.33×10^{-1}	30000

The mechanical partial molar proprerties were computed according to the fluctuation-explicit operational definitions [Equations (2) and (3)], as follows: for each pairwise fluctuation, $\langle \delta x \delta y \rangle$, cumulative sums of instantaneous values of x, y, and xy were updated at each step in the simulation, and for each one of the eight space-filling control volumes into which the periodic box was divided. The required pairwise fluctuation was calculated by averaging the accumulated sums over all control volumes and over the total number of steps, and computing the quantity $\langle \delta x \delta y \rangle$ as $\langle xy \rangle - \langle x \rangle \langle y \rangle$ (the particular pairwise fluctuations included in Figures 4 and 5 are extensive: reported numbers are per control volume). In addition, the time evolution of $\langle \delta x \delta y \rangle$ was monitored by computing the quantity $\langle xy \rangle - \langle x \rangle \langle y \rangle$ several times over the course of a run: Figures 1 and 4 were obtained in this way. Calculated properties are for the shifted-force binary Lennard-Jones mixtures in all cases.

To calculate the error estimates for $\bar{U}_i$ and $\bar{V}_i$ reported in Table 3, the partial molar properties were computed at ten different times during the simulation (see Figures 1 and 4). Standard deviations were then calculated over the last few values (typically 5, never less than three), after the initial transients (see Figure 1 and 4) disappeared. Enthalpy errors were calculated from the equation

$$|\Delta \bar{H}_i| = \bar{V}_i|\Delta P| + P|\Delta \bar{V}_i| + |\Delta \bar{U}_i| + |\Delta P \Delta \bar{V}_i| \qquad \text{(A2-3)}$$

In (N, U, V) molecular dynamics, uncertainties in the computed partial molar enthalpies are dominated by pressure fluctuations. The latter, as well as temperature fluctuations were obtained from the quantities $\langle P^2 \rangle - \langle P \rangle^2$, $\langle T^2 \rangle - \langle T \rangle^2$, with averages computed over every step in the simulation. The number of space-filling control volumes used in this work was 8. Each control volume therefore contained, on average, 32 molecules. It has already been shown [9] that for $N = 256$, calculated partial molar properties are insensitive to a change in the number of control volumes from 8 to 16. Pair correlation functions shown in Figures 9, 13, and 14 were obtained by averaging 5000 "snapshots". The separation range $0 < r < 0.8661$ was sampled in 200 increments of width $4.33 \times 10^{-3} l$; the method of Theodorou and Suter [16] was used to extend the range of r beyond half a periodic box length $(l/2)$.

All simulations followed equilibration runs in which the system was started from a face-centered cubic structure, with solute molecules randomly placed within the regular lattice. A unimodal velocity distribution $(3T^*/m_i^*)^{1/2}$ with randomly oriented components was imposed upon each species. T^* is an "objective" temperature from which the system was started, and towards which it was brought during the equilibration run by time rescaling [see Equation (A2-2)]. This "thermostatting" procedure can, in theory, lead to numerical instabilities (since velocities are reduced by increasing the time step), but this problem was never encountered in this work. The time step used in the actual simulation, therefore, varied from run to run (see Table A2.1) and corresponded to the last time step used during equilibration (several hundred steps elapsed between the last time rescaling and the end of the equilibration run). Equilibration runs varied in length, but were never shorter than $t^* = 10$ (based on the nomimal, initial time step), to guarantee the system's complete memory loss vis-à-vis its initial configuration.

References

[1] C.A. Eckert, D.H. Ziger, K.P. Johnston, and T.K. Ellison, "The Use of Partial Molar Data to Evaluate Equations of State for Supercritical Fluid Mixtures," *Fluid Phase Equil.*, **14**, 167 (1983).

[2] C.A. Eckert, D.H. Ziger, K.P. Johnston, and S. Kim, "Solute Partial Molal Volumes in Supercritical Fluids," *J. Phys. Chem.*, **86**, 2738 (1986).

[3] K.S. Shing and T.S. Chung, AIChE Annual Meeting, Miami, November 1986, paper 64C.

[4] J. Owicki and H. Scheraga, "Monte Carlo Simulations in the Isothermal-Isobaric Ensemble. 2. Dilute Aqueous Solution of Methane," *J. Am. Chem. Soc.*, **99**, 7413 (1977).

[5] G. Bolis and E. Clementi, "Methane in Aqueous Solution at 300 K," *Chem. Phys. Lett.*, **82**, 147 (1981).

[6] P.G. Debenedetti, "Clustering in Dilute, Binary Supercritical Mixtures: a Fluctuation Analysis," *Chem. Eng. Sci.*, **42**, (9), 2203 (1987).

[7] P.G. Debenedetti and S.K. Kumar, "The Molecular Basis of Temperature Effects in Supercritical Extraction," *AIChEJ*, **34**(4), 645 (1988).

[8] M. Modell and R.C. Reid, *Thermodynamics and its Applications*, 2nd edition, Prentice-Hall, Englewood Cliffs, NJ, 1983, pp. 182–184.

[9] P.G. Debenedetti, "Fluctuation-based Computer Calculation of Partial Molar Properties. I. Molecular Dynamics Simulation of Constant Volume Fluctuations," *J. Chem. Phys.*, **86**(12), 7126 (1987).

[10] P.G. Debenedetti, "Fluctuation-based Computer Calculation of Partial Molar Properties. II. A Numerically Accurate Method for the Determination of Partial Molar Energies and Enthalpies," *J. Chem. Phys.*, **88**(4), 2681 (1988).

[11] J.G. Kirkwood and F.P. Buff, "The Statistical Mechanical Theory of Solutions. I,"*J. Chem. Phys.*, **19**(6), 774 (1951).

[12] A.Z. Panagiotopoulos, "High Pressure Phase Equilibria: Experimental and Monte Carlo Simulation studies," Ph.D. Thesis, Massachusetts Institute of Technology, Cambridge, MA (1986).

[13] W.B. Streett, D.J. Tildesley, and G. Saville, "Multiple Time Step Methods and an Improved Potential Function for Molecular Dynamics Simulations of Molecular Liquids," in *Computer Modelling of Matter*, ACS Symp. Ser. **86**, P. Lykos, ed., American Chemical Society, Washington, DC (1978), ch. 13.

[14] A.Z. Panagiotopoulos, U.W. Suter, and R.C. Reid, "Phase Diagrams of Nonideal Mixtures from Monte Carlo Simulation," *Ind. Eng. Chem. Fundam.*, **25**, 525 (1986).

[15] P.G. Debenedetti, "The Statistical Mechanical Theory of Concentration Fluctuations in Mixtures," *J. Chem. Phys.*, **87**, 1256 (1987).

[16] D.N. Theodorou and U.W. Suter, "Geometrical Considerations in Model Systems with Periodic Boundaries," *J. Chem. Phys.*, **82**(2), 955 (1985).

[17] K.P. Shukla, "Thermodynamic Properties of Simple Fluid Mixtures from Perturbation Theory," *Molec. Phys.*, **62**(5), 1143 (1987).

[18] L. Verlet, "Computer 'Experiments' on Calssical Fluids. I. Thermodynamical Properties of Lennard-Jones Molecules," *Phys. Rev.*, **159**(1), 98 (1967).